Received: 10 June 2024 | Revised: 25 September 2024 | Accepted: 6 November 2024

DOI: 10.1002/pro.5225

RESEARCH ARTICLE

THE PROTEIN SOCIETY WILEY

Distinct substrate specificities of the three catalytic subunits of the *Trichomonas vaginalis* proteasome

Pavla Fajtova[1,2,3] | **Brianna M. Hurysz**[1,3] | **Yukiko Miyamoto**[3,4] | **Mateus Sá M. Serafim**[1,3,5] | **Zhenze Jiang**[1,3] | **Julia M. Vazquez**[1,3] | **Diego F. Trujillo**[1,3] | **Lawrence J. Liu**[1,3] | **Urvashi Somani**[1,3] | **Jehad Almaliti**[3,6] | **Samuel A. Myers**[7] | **Conor R. Caffrey**[1,3] | **William H. Gerwick**[1,3,6] | **Dustin L. McMinn**[8] | **Christopher J. Kirk**[8] | **Evzen Boura**[2] | **Lars Eckmann**[3,4] | **Anthony J. O'Donoghue**[1,3]

[1]Skaggs School of Pharmacy and Pharmaceutical Sciences, University of California San Diego, La Jolla, California, USA

[2]Institute of Organic Chemistry and Biochemistry of the Czech Academy of Sciences, Prague 6, Czech Republic

[3]Center for Discovery and Innovation in Parasitic Diseases, Skaggs School of Pharmacy and Pharmaceutical Sciences, University of California, La Jolla, California, USA

[4]Department of Medicine, University of California San Diego, La Jolla, California, USA

[5]Departamento de Microbiologia, Instituto de Ciências Biológicas, Universidade Federal de Minas Gerais (UFMG), Belo Horizonte, Minas Gerais, Brazil

[6]Scripps Institution of Oceanography, University of California San Diego, La Jolla, California, USA

[7]Division of Signaling and Gene Expression, La Jolla Institute for Immunology, La Jolla, California, USA

[8]Kezar Life Sciences, South San Francisco, California, USA

Correspondence
Anthony J. O'Donoghue, Skaggs School of Pharmacy and Pharmaceutical Sciences, University of California San Diego, La Jolla, CA 92093, USA.
Email: ajodonoghue@health.ucsd.edu

Funding information
HORIZON EUROPE Marie Sklodowska-Curie Actions, Grant/Award Number: 846688; St. Baldrick's Foundation; Universidade Federal de Minas Gerais; Coordenação de Aperfeiçoamento de Pessoal de Nível Superior, Grant/Award Numbers: 88887.595578/2020-00, 88887.684031/2022-00; National Institutes of Health, Grant/Award Numbers: R01 AI158612, R21 AI146387, R21 AI133393, R21 AI171824, DK120515; Akademie Věd České Republiky, Grant/Award Number: MSM200551901; National Institute of General Medical Sciences, Grant/Award Number: T32GM007752

Abstract

The protozoan parasite *Trichomonas vaginalis* (Tv) causes trichomoniasis, the most common non-viral sexually transmitted infection in the world. Although Tv has been linked to significant health complications, only two closely related 5-nitroimidazole drugs are approved for its treatment. The emergence of resistance to these drugs and lack of alternative treatment options poses an increasing threat to public health, making development of novel anti-*Trichomonas* compounds an urgent need. The proteasome, a critical enzyme complex found in all eukaryotes has three catalytic subunits, β1, β2, and β5 and has been validated as a drug target to treat trichomoniasis. With the goal of developing tools to study the Tv proteasome, we isolated the enzyme complex and identified inhibitors that preferentially inactivate either one or two of the three catalytic subunits. Using a mass spectrometry-based peptide digestion assay, these inhibitors were used to define the substrate preferences of the β1, β2 and β5 subunits. Subsequently, three model fluorogenic substrates were designed, each specific for one of the catalytic subunits. This novel substrate profiling methodology will allow for individual subunit characterization of other

Pavla Fajtova and Brianna M. Hurysz contributed equally to this study.

Review Editor: John Kuriyan

proteasomes of interest. Using the new substrates, we screened a library of 284 peptide epoxyketone inhibitors against Tv and determined the subunits targeted by the most active compounds. The data show that inhibition of the Tv β5 subunit alone is toxic to the parasite. Taken together, the optimized proteasome subunit substrates will be instrumental for understanding the molecular determinants of proteasome specificity and for accelerating drug development against trichomoniasis.

KEYWORDS

drug discovery, drug screening, parasite, protease inhibitor, proteasome, substrate specificity, trichomonas

1 | INTRODUCTION

Trichomonas vaginalis (Tv) is the protozoan parasite responsible for the most common non-viral sexually transmitted infection, trichomoniasis (Kissinger 2015; Petrin et al. 1998). Trichomoniasis can cause various symptoms including vaginal discharge, irritation, and itchiness. The infection can be asymptomatic and has historically been disregarded as a serious threat to human health, therefore, diagnosis and treatments are understudied (Menezes et al. 2016; Schwebke and Burgess 2004). However, comorbidity with other sexually transmitted infections as well as the relationship with other serious health concerns including cancers, HIV acquisition, infertility, and adverse pregnancy outcomes points to a need for improved diagnostic and therapeutic options (Kissinger 2015; Petrin et al. 1998; Schwebke and Burgess 2004). Due to a lack of screening for trichomoniasis, incidence estimates range widely from 156 to 276 million annual cases worldwide (Cates 1999; Menezes et al. 2016; Rowley et al. 2019).

The 5-nitroimidazole drugs, metronidazole and tinidazole, are the only two FDA approved drugs for treatment of trichomoniasis. Nitroimidazoles are prodrugs that require activation by nitro group reduction in anaerobic microbes, leading to the generation of reactive intermediates that form cytotoxic protein adducts (Dingsdag and Hunter 2018). While metronidazole and tinidazole are generally effective for treating trichomoniasis, significant adverse effects can occur, including nausea, abdominal pain, diarrhea, metallic taste, neurotoxicity, and optic neuropathy (Hernández Ceruelos et al. 2019). Oral metronidazole treatment also impacts the gut microbiome with potential long-term health impacts. In a murine model, metronidazole was linked to a reduction of probiotic related bacterial communities and development of antibiotic-resistant bacteria (Huang et al. 2022). In healthy dogs, metronidazole decreased microbiome richness and reduced abundance of key bacteria that did not recover 4 weeks after discontinuing treatment (Pilla et al. 2020). Lastly, Tv strains with resistance to metronidazole are becoming more prevalent, with some studies estimating resistance rates as high as 9.6% (Cudmore et al. 2004; Hernández Ceruelos et al. 2019; Narcisi and Secor 1996; Schwebke and Barrientes 2006). The high incidence of Tv infection paired with limited diagnostics, its correlation to other serious health impairments, growing resistance to drugs, and the potential deleterious effects of current drugs on the gut microbiome, make the development of new trichomoniasis drugs urgent.

In eukaryotes, the 20S proteasome is responsible for proteolysis in the ubiquitin-dependent protein degradation pathway. This process of degrading damaged, misfolded, or unneeded proteins is necessary for eukaryotes to maintain homeostasis. In addition, the human proteasome degrades proteins into peptides that are presented as antigens on the cell surface by the major histocompatibility complex (Vigneron and Van den Eynde 2014). The 20S proteasome has a hollow cylindrical structure consisting of a stack of four heptameric rings, each composed of either seven α subunits, α1 to α7, in the outer rings or seven β subunits, β1–β7, in the two inner rings (Budenholzer et al. 2017; Collins and Goldberg 2017). The β rings contain three catalytic subunits, β1, β2, and β5, each with distinct substrate specificity. Subunit-specific fluorogenic substrates of the human proteasome have been used extensively as reporters of activity from each subunit (Liggett et al. 2010) to screen compound collections for proteasome inhibitors, and to uncover the mechanism of inhibitor binding (Kisselev 2022).

We previously validated the 20S proteasome (Tv20S) as a drug target in Tv infections (O'Donoghue et al. 2019) using proteasome inhibitors that are clinically approved for treating cancers such as multiple myeloma (Manasanch and Orlowski 2017). Currently approved proteasome inhibitors are likely to be too toxic for treatment of

parasitic diseases such as trichomoniasis and therefore Tv-specific proteasome inhibitors with low human cell cytotoxicity are needed to realize the potential of this therapeutic approach. Only few bacterial species have a proteasome and therefore, a selective, potent and effective proteasome inhibitor against Tv would likely have fewer, if any, negative impacts on the gut microbiome when compared to nitroimidazole drugs, which target a broad spectrum of anaerobic microbes (Becker and Darwin 2016).

Inhibition of protozoan proteasomes has recently become an established strategy for drug development. Active site differences between the human and parasite 20S proteasome have been exploited to develop inhibitors that specifically target the parasite proteasome (Bibo-Verdugo et al. 2019; Koester et al. 2022; Krishnan and Williamson 2018; LaMonte et al. 2017; Li et al. 2016; Nagle et al. 2020a; Wyllie et al. 2019a; Xie et al. 2019; Zhang and Lin 2021). For example, proteasome inhibitors were developed that are >2,000-fold more toxic to *Plasmodium falciparum* than human cells (LaMonte et al. 2017). In addition, two related proteasome inhibitors are currently in clinical trials for treatment of visceral leishmaniasis (Nagle et al. 2020b; Wyllie et al. 2019b). These studies with other protozoan parasites encouraged us to define the enzymatic activity of the proteasome from Tv with the goal of revealing the substrate specificity of Tv20S and uncovering the role that each of the catalytic subunits play in substrate digestion. The knowledge gained will improve the understanding of Tv20S function while also providing new guidance on how to design reporter substrates and proteasome inhibitors.

2 | RESULTS

2.1 | Isolation and subunit identification of Tv20S proteasome

To perform an in-depth characterization of Tv20S and define the substrate specificity of the catalytic Tv proteasome subunits, we first isolated Tv20S from protein extracts using sequential steps of ammonium sulfate precipitation, size exclusion chromatography and anion exchange chromatography (Figure S1, Supporting Information). At each step, catalytic activity was evaluated using the fluorogenic substrate, Suc-Leu-Leu-Val-Tyr-7-amino-4-methylcoumarin (Suc-LLVY-amc), which is cleaved by Tv20S as well as several other eukaryotic proteasomes (Becker and Darwin 2016; Bibo-Verdugo et al. 2017; Jalovecka et al. 2018; O'Donoghue et al. 2019; Saha et al. 2020; Tanaka 2009; Vigneron and Van den Eynde 2014; Zhang and Lin 2021). Visualization of the isolated Tv20S by non-denaturing, native gel electrophoresis and silver staining revealed a protein complex of ~700 kDa (Figure 1a), which was smaller than the ~750 kDa of the human constitutive 20S proteasome (c20s) analyzed in parallel (Tanaka 2009). These findings are consistent with the calculated masses of Tv20S (697.3 kDa) and c20S (716.4 kDa) as predicted from the respective genomes (Data S1). To confirm that the isolated protein was Tv20S, it was incubated with a proteasome-specific activity-based probe, Me4BodipyFL-Ahx3Leu3VS, consisting of a tri-leucine-vinyl sulfone inhibitor and an N-terminal fluorescent tag (Berkers et al. 2007) The enzyme-probe complex was resolved by non-denaturing gel electrophoresis and visualized by fluorescent imaging. The probe bound to a single band which corresponded to the silver-stained band of the isolated Tv20S (Figure 1a,b). These results demonstrate that catalytically active Tv20S can be isolated from Tv lysate.

To determine which Tv20S subunits are labeled by the fluorescent probe, we incubated the isolated Tv20S with the probe for various times and separated the individual subunits by SDS-PAGE (Figure 1c). The probe

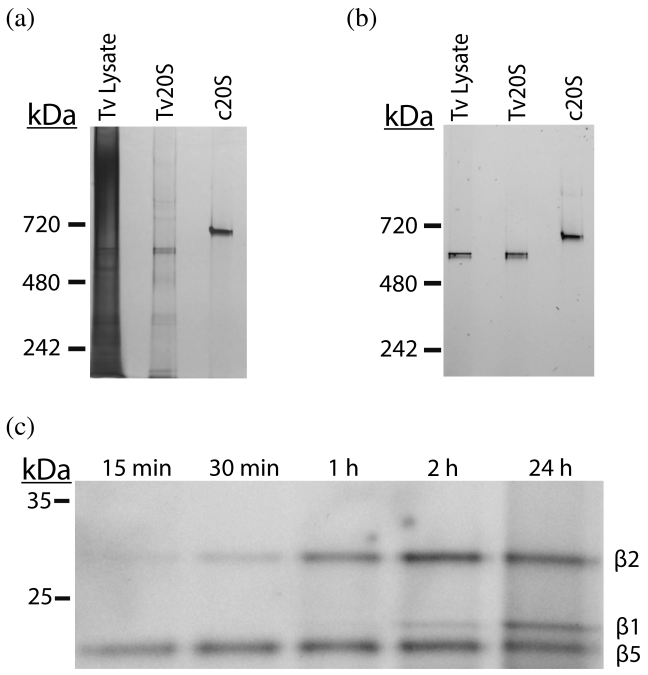

FIGURE 1 Gel electrophoresis-based characterization of Tv20S. (a) Tv lysate, isolated Tv20S, and human c20S were resolved on a non-denaturing NuPAGE 3%–8% tris-acetate gel, silver stained and imaged. (b) The same protein samples were incubated for 1 h with 2 μM of the fluorescent Me4BodipyFL-Ahx3Leu3VS probe and imaged with 470 nm excitation and 530 nm emission wavelengths. (c) Tv lysate was incubated with 2 μM of the fluorescent probe for the indicated times and the subunits were resolved by electrophoresis using a NuPAGE 12% bis-tris denaturing gel.

labeled two bands at ~20 and ~30 kDa within 1 h, and a third band with an intermediate molecular weight of ~23 kDa after >2 h incubation. These findings indicate that the probe detects three catalytic Tv20S subunits in a time-dependent manner, requiring up to 24 h incubation for strong labeling. The three bands were excised from the SDS-PAGE gel and subjected to proteomic analysis. The most abundant proteasome subunit found in the upper (~30 kDa) band was the Tv protein, UniProt A2F2T6 while the middle (~23 kDa) and lower (~20 kDa) bands were determined to be the proteins, UniProt A2E7Z2 and A2DD57 (Figure S2). The genomic sequences of these proteins align >40% with each of the respective human catalytic subunits β2 (UniProt Q99436), β1 (UniProt P28072), and β5 (UniProt P28074), and therefore were assigned as follows: β2 (UniProt A2F2T6), β1 (UniProt A2E7Z2), and β5 (UniProt A2DD57) (O'Donoghue et al. 2019). Although the probe only labels catalytic subunits, several non-catalytic proteasome subunits and putative proteasome binding proteins were also detected in the excised gel fragments, consistent with their predicted sizes within the range of the catalytic subunits.

2.2 | Tv20S subunit inactivation with irreversible inhibitors

Using the fluorescent probe to visualize the catalytic subunits of Tv20S, we evaluated previously identified proteasome inhibitors for their ability to inactivate one or more of the subunits. Tv20S was pre-incubated with 1 μM of the proteasome inhibitor, carmaphycin-17 (CP-17) (O'Donoghue et al. 2019) for 1 h, prior to labeling with the fluorescent probe and showed a concentration-dependent decrease in labeling of all three subunits. A one-sample *t*-test was performed with a Bonferroni alpha value correction for multiple tests to assess if the intensity of any bands were significantly reduced ($p < 0.00278$). Using 2 μM of CP-17, β5 is significantly reduced, while β5 and β2 are both significantly reduced in the presence of 5 μM CP-17 (Figure 2a,b). Using 5 μM of carfilzomib (CFZ), β5 and β2 are significantly reduced (Figure 2c,d). Therefore, we conclude that CP-17 preferentially inhibits the β5 subunit of Tv20S whereas CFZ inhibits both β2 and β5, making these two inhibitors valuable tools for biochemical characterization of Tv20S substrate specificity.

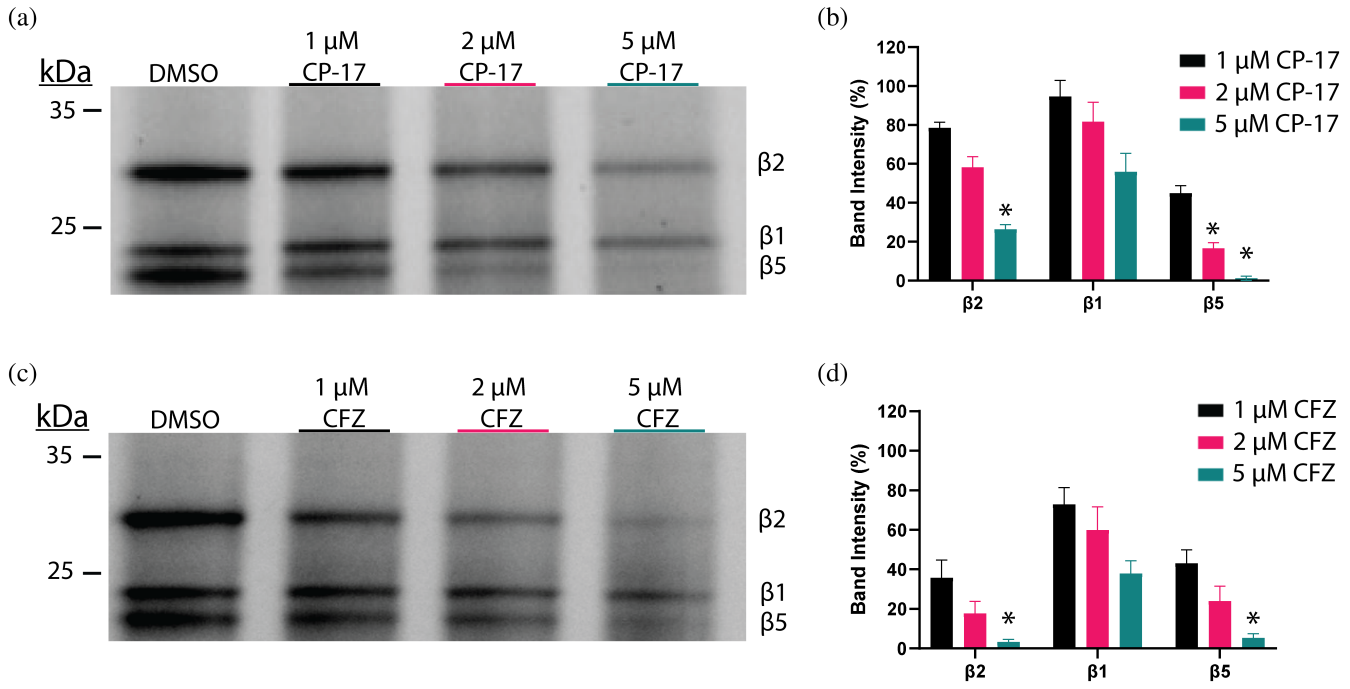

FIGURE 2 Subunit-specific inhibition of Tv20S by carmaphycin-17 (CP-17) and carfilzomib (CFZ). Tv20S was preincubated with 1–5 μM of CP-17 (a) or CFZ (c) for 1 h prior to labeling with the Me4BodipyFL-Ahx3Leu3VS probe and size separation by SDS-PAGE gel electrophoresis. The bands from (a) and (c) were respectively quantified with ImageJ software (b, d), and the intensities were plotted relative to the band intensity in vehicle (DMSO) treated lanes. Three independent assays were performed using the same preparation of Tv20S. Results represent means and SEM of the triplicate assays and * represents band intensity that is significantly changed relative to the non-inhibitor treated control.

2.3 | Substrate specificity of Tv20S catalytic subunits

To define the substrate specificity of Tv20S, we employed multiplex substrate profiling by mass spectrometry (MSP-MS) (Lapek et al. 2019; Rohweder et al. 2022), a method that was previously used to determine the substrate specificity of the human and *Plasmodium falciparum* proteasomes (Li et al. 2016; Winter et al. 2017). This method employs the use of 228 strategically designed peptides which contain all possible combinations of amino acids surrounding a cleavage site. Following incubation of the enzyme with this peptide mixture, quantification of the cleaved products by liquid chromatography, and tandem mass spectrometry (LC–MS/MS) revealed that Tv20S cleaved 165 of 2964 available peptide bonds after a 20 h incubation (Data S2). Of these cleavage sites, 90% were located between the 4th and 12th amino acid, indicating that Tv20S strongly favors cleaving at sites that are not adjacent to the N- and C-termini (Figure 3a). Based on the detected cleavage sites, we generated an iceLogo plot to illustrate the frequency of amino acids occurring in each of the eight P4 to P4′ positions (Figure 3b). The profile revealed that hydrophobic amino acids (particularly F and P) were found most frequently in P4 and P4′. At P3, a high frequency of hydrophobic residues was also observed, in addition to the positively charged residues, R and H. At P2, H and K were preferred, and P was not well tolerated. At P1, N, R, and F were commonly found, while peptides were generally not cleaved when P, G, T, K, and Q were in the P1 position. These data demonstrate that the Tv proteasome is an endopeptidase that cleaves a wide range of peptide bonds but with distinct preferences for the amino acids adjacent to the cleavage site.

To characterize the cleavage profile of individual subunits of Tv20S, we preincubated the enzyme with different combinations and concentrations of the irreversible inhibitors CP-17 and CFZ to preferentially inactivate either β5 alone (1 μM CP-17), and both β5 and β2 (10 μM of CP-17 or 10 μM of CP-17 and 10 μM of CFZ). These concentrations were chosen based on our preliminary studies using Suc-LLVY-amc and Boc-LRR-amc which revealed that 1 μM of CP-17 decreases β5 activity (Suc-LLVY-amc) by 89% while only reducing β2 activity (Boc-LRR-amc) by 23% (Figure S3). At 10 μM of CP-17 and in the presence of CFZ, β2 activity was reduced by 98%. The abundance of each cleaved product in the MSP-MS analysis was compared between the inhibitor-treated preparation relative to the vehicle-treated control (2.5% DMSO). From the normalized data, we performed a hierarchical clustering analysis and found that three distinct groups of cleaved peptides were generated from the different assay conditions (Figure 3c). Group 1 cleavage sites were

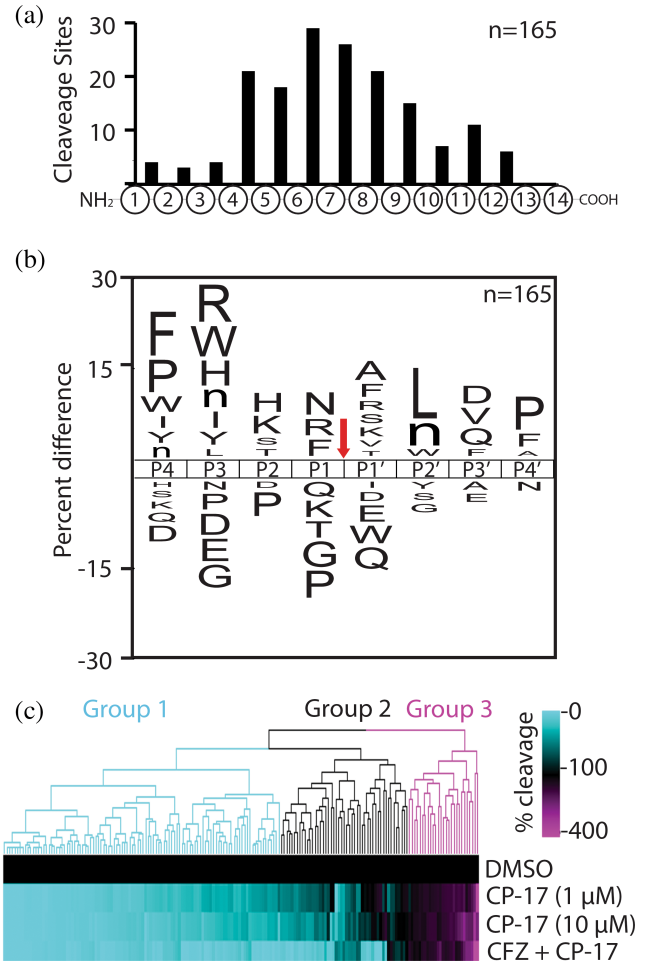

FIGURE 3 Characterization of peptides cleaved by Tv20S. (a) Distribution of cleavage sites within the 14-mer peptides. (b) IceLogo frequency plot of the peptides cleaved by Tv20S showing the amino acids that are increased (above mid-line) and decreased (below mid-line) in the P4 to P4′ positions. The red arrow indicates the cleavage site. Lowercase n in the plot designates norleucine. (c) Abundance of individual cleaved peptides is expressed as a percentage relative to their abundance in DMSO treated controls. Cyan colors designate peptides whose cleavage was decreased by the indicated inhibitors, while purple colors depict peptides that were more abundant in the presence of the inhibitors compared to DMSO controls. Cleavage products clustered into three main groups, designated as 1 to 3.

related to β5 activity, because the formation of these cleavage products was significantly decreased in the presence of CP-17. Group 2 corresponded to β2 activity as the cleavage products were reduced by 10 μM of CP-17 and CFZ but not by 1 μM of CP-17. Group 3 consisted of cleavage products that were not reduced in the presence of CP-17 and CFZ when compared to the vehicle control. These cleavage products are likely to have been generated by β1, the remaining third catalytic subunit. In summary, the cleaved peptides generated by Tv20S activity could be

clustered into three groups, which correlated with the three catalytic subunits.

2.4 | Development of a β5-specific Tv20S substrate

We next leveraged the cleavage and inhibition profiles to develop subunit-specific reporter substrates. Using 1 μM of CP-17, we had shown above that only Tv20S β5 is inactivated (Figure 2a). In the MSP-MS studies, Group 1 consisted of cleaved peptides that were reduced in abundance when Tv20S was treated with 1 μM CP-17 (Figure 3c). Therefore, Group 1 peptides are the products of the β5 subunit. An iceLogo of the 96 cleavage sites of the Group 1 peptides revealed that this subunit preferentially hydrolyzes substrates with hydrophobic amino acids in the P4, P1, and P4′ positions and mixed types of amino acids in other positions (Figure 4a). In the P3 position the most frequent residues found were W, R, and H, with W being the most enriched amino acid at any of the P4 to P4′ positions. The fluorogenic substrate that we had previously used for detecting activity of Tv20S β5 consists of the P4 to P1 sequence, LLVY (O'Donoghue et al. 2019). This substrate was developed for c20S, but based on the iceLogo, Y in the P1 position appears to be the only amino acid in this substrate that is preferred by Tv20S. Therefore, we chose a new peptide from the MSP-MS substrate library (AnTDRGWYL*AIQAV) that contains W in P3 and was cleaved with high efficiency by Tv20S between L and A (Figure 4b). The cleavage product (AnTDRGWYL) was not formed in the presence of 1 μM CP-17, confirming that it is a substrate of β5. Using the P4 to P1 sequence as a template, we synthesized a fluorogenic substrate, Ac-GWYL-amc, consisting of the tetrapeptide flanked by an N-terminal acetyl (Ac) capping group and a C-terminal fluorescent amc reporter group. The cleavage of this substrate, evaluated using a concentration range of 2–250 μM, was characterized by a K_M of 7.41 ± 1.73 μM (Figure 4c). Under identical conditions, the K_M for the human β5 substrate, Suc-LLVY-amc, was determined to be 589.4 ± 134.7 μM. Thus, Ac-GWYL-amc is cleaved with ∼80-fold higher affinity than Suc-LLVY-amc.

2.5 | Development of a β2-specific substrate

We next evaluated the peptides in cleavage Group 2 whose abundance was partially reduced by 1 μM of CP-17 and further reduced with 10 μM of CP-17 or a combination of 10 μM CP-17 and 10 μM CFZ (Figure 3c). Since these conditions led to inhibition of both β5 and β2 and we had already resolved Group 1 as β5 cleavages, Group 2 cleavages were attributed to β2 activity (Figure 3c). The iceLogo plot of the 48 peptides in Group 2 revealed that the β2 subunit prefers peptides with hydrophobic amino acids at P4, and R at both P3 and P1 (Figure 5a). We chose HWAFRSR*YHGPLAH from the MSP-MS substrate library as a template for designing a β2 substrate as it closely matched the consensus sequence. Cleavage of this substrate was inhibited in a concentration-dependent manner by CP-17 with full inhibition seen with a combination of CP-17 and CFZ (Figure 5b). Consequently, based on the core tetrapeptide FRSR, we synthesized a fluorogenic substrate, Ac-FRSR-amc, and used it for assaying Tv20S. A concentration-response resulted in a

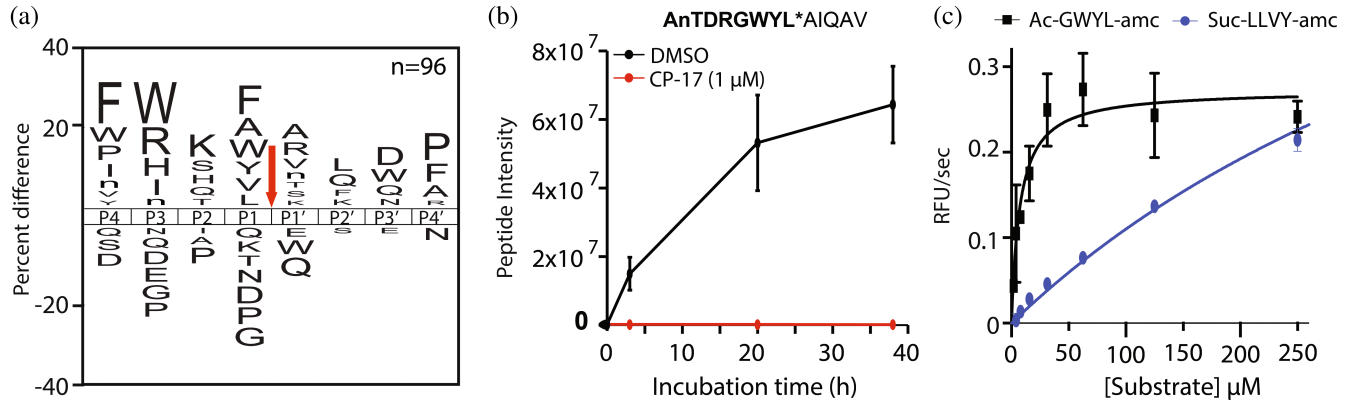

FIGURE 4 Design of a Tv20S β5-specific substrate. (a) IceLogo frequency plot showing the amino acids that are increased (above mid-line) and decreased (below mid-line) in the P4 to P4′ positions of the Tv20S β5 subunit. Lowercase n corresponds to norleucine. (b) Example peptide from the MSP-MS substrate library that is cleaved by Tv20S and whose cleavage is inhibited by 1 μM CP-17 (mean ± SE, $n = 4$ replicates). The N-terminal cleavage product in bold was identified by LC–MS/MS. (c) Michaelis Menten plots with the indicated fluorogenic substrates (mean ± SE, $n = 3$ replicates).

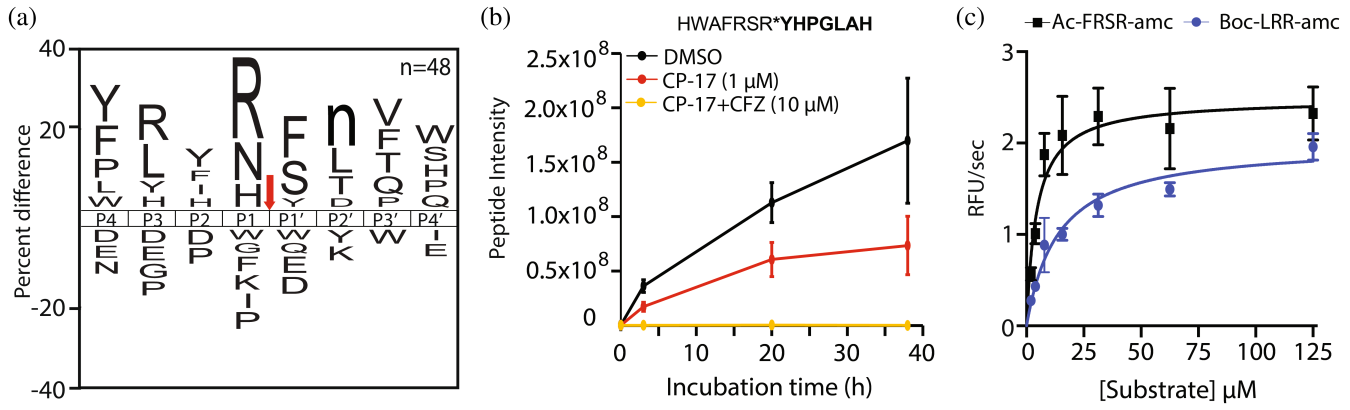

FIGURE 5 Design of a β2-specific substrate. (a) IceLogo frequency plot showing the amino acids that are increased (above mid-line) and decreased (below mid-line) in the P4 to P4′ positions of the Tv20S β2 subunit. Lowercase n corresponds to norleucine. (b) Example peptide that is cleaved by Tv20S, partially inhibited by 1 μM CP-17, and fully inhibited by 10 μM each of CP-17 and CFZ. The cleavage product in bold was identified via LC–MS/MS (mean ± SE, $n = 4$ replicates). (c) Michaelis Menten plot with the substrates Ac-FRSR-amc and Boc-LRR-amc (mean ± SE, $n = 3$ replicates).

calculated K_M of 4.39 ± 1.0 μM (Figure 5c). Under identical conditions, the K_M for the human β2 substrate, Boc-LRR-amc, was 13.72 ± 2.36 μM. Ac-FRSR-amc is therefore a higher affinity reporter substrate than the standard human substrate for monitoring β2 activity of Tv20S.

2.6 | Development of a β1-specific Tv20S substrate

Finally, we evaluated peptides in cleavage Group 3 that were not inhibited by the combination of 10 μM CP-17 and 10 μM CFZ and, in many cases, the intensity of the cleaved products increased in the presence of these inhibitors (Figure 3c). Based on these properties, we concluded that these peptides were most likely hydrolyzed by the β1 subunit or possibly other protease(s) that may have been enriched during the isolation of Tv20S. The iceLogo plot of the 27 cleavage sites in this group revealed that most had either D, N, or E in the P1 position (Figure 6a), and one of the most efficiently cleaved peptides in the MSP-MS substrate library was QYELPSRN*GWHHNP (Figure 6b). Consequently, the tetrapeptide sequence, PSRN, corresponding to the P4-P1 amino acids was synthesized with a fluorogenic reporter to yield Ac-PSRN-amc. As expected, this fluorogenic substrate was cleaved by Tv20S and the activity was not significantly inhibited by CP-17 or a combination of CP-17 and CFZ (Figure 6c). This lack of inhibition revealed that Ac-PSRN-amc is cleaved by an enzyme that is distinct from the Tv20S β5 and β2 subunits. However, cleavage of peptides with asparagine in the P1 position is uncharacteristic of other proteasomes (Harris et al. 2001), and these data did not sufficiently confirm that cleavage of Ac-PSRN-amc was the result of Tv20S β1 activity.

We next evaluated an alternative proteasome inhibitor, bortezomib (BTZ), which is known to inactivate the β1 subunit of the human proteasome and several microbial proteasomes (Buac et al. 2013; Collins et al. 2010; Piro et al. 2012; Reynolds et al. 2007). Tv lysate was pre-incubated with 2, 5, and 10 μM of BTZ prior to labeling with the fluorescent probe, Me4BodipyFL-Ahx3Leu3VS. These assays showed that BTZ targets the β1 subunit of Tv20S (Figure S4). However, when BTZ was incubated with Tv20S and assayed using Ac-PSRN-amc, no inhibition of activity was observed. This revealed that the enzyme responsible for hydrolyzing Ac-PSRN-amc is not Tv20S β1. Meanwhile asparagine is known to be the preferred P1 amino acids for the legumain family of cysteine proteases, such as Tv legumain 1 (TvLEGU-1), an abundant Tv protease that is known to hydrolyze the tripeptide substrate Z-AAN-amc (Rendón-Gandarilla et al. 2013). Therefore, we speculated that the cleavage of Ac-PSRN-amc may be due to the presence of a contaminating legumain such as TvLEGU-1. We anticipated that cleavage of substrates with asparagine at P1 would be inhibited by RR11a, a well characterized azapeptidyl inhibitor of legumain (Ekici et al. 2004; Götz et al. 2008; León-Félix et al. 2004; Rendón-Gandarilla et al. 2013). We found that Ac-PSRN-amc and Z-AAN-amc activities were inhibited by RR11a, demonstrating TvLEGU-1 or a related enzyme co-purified with Tv20S (Figure 6c).

Having determined that Ac-PSRN-amc is not a β1 substrate, we subsequently selected a different peptide from the MSP-MS substrate library, EPLDLQKQ-RYFD*WL, one of the most efficiently cleaved peptides in Group 3 that did not have a P1-N residue, as an

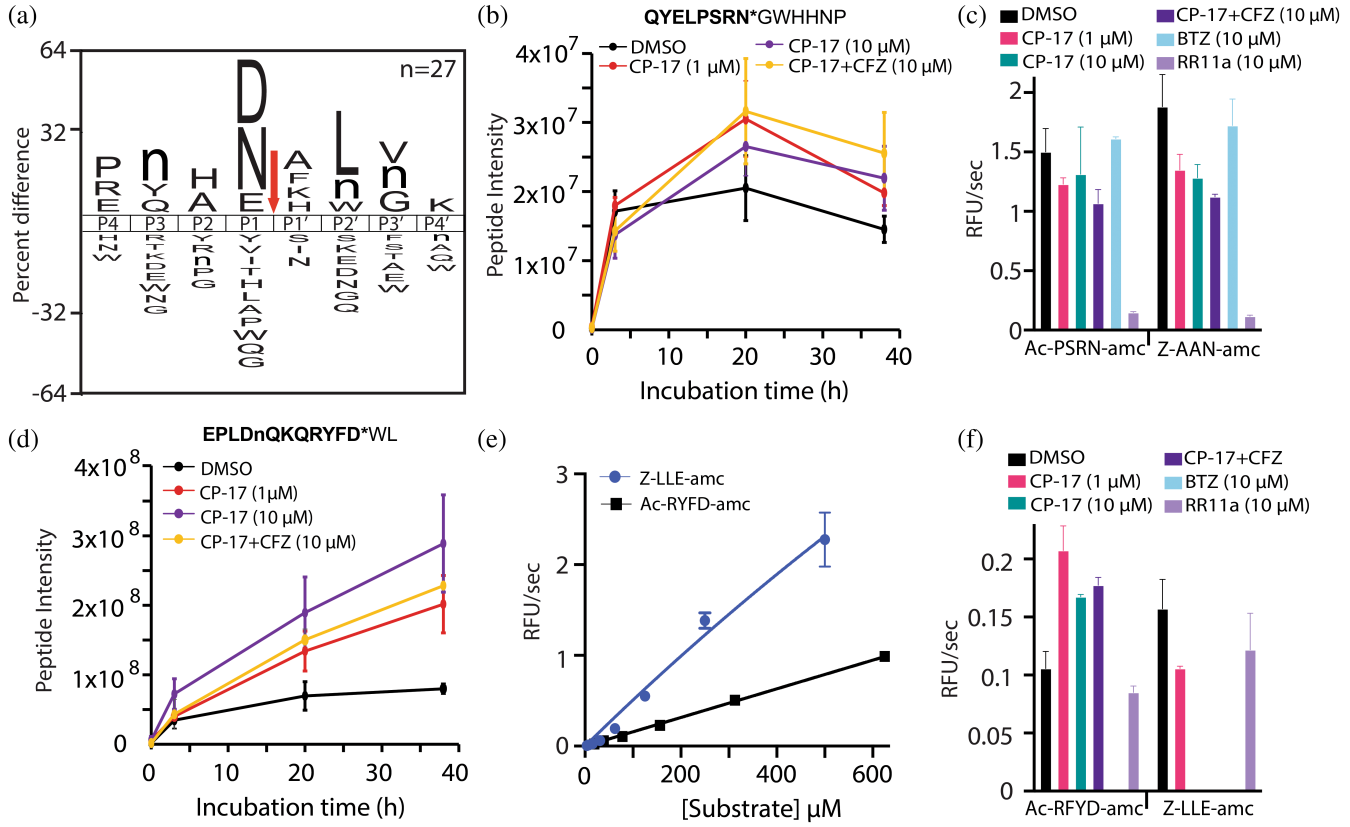

FIGURE 6 Design of a β1-specific substrate. (a) IceLogo frequency plot showing the amino acids that are increased (above mid-line) and decreased (below mid-line) in the P4 to P4′ positions of cleaved peptides in Group 3. Lowercase *n* corresponds to norleucine. (b) Example peptide product that is cleaved independent of CP-17 and/or CFZ ($n = 4$). (c) Enzyme activity using Ac-PSRN-amc and the legumain substrate Z-AAN-amc ($n = 3$). (d) Example peptide product that is cleaved by Tv20S β1 where activity increases in the presence of CP-17 and CFZ (mean ± SE, $n = 4$ replicates). (e) Michaelis Menten plot of Ac-RYFD-amc and Z-LLE-amc (mean ± SE, $n = 3$ replicates). (f) Enzyme activity using Ac-RYFD-amc and Z-LLE-amc following a 30 min preincubation of Tv20S with the indicated inhibitors (mean ± SE, $n = 3$ replicates).

alternative template for a β1 substrate (Figure 6d). Interestingly, the cleavage products of this peptide were increased in the presence of CFZ and CP-17 which would indicate that these compounds are activating enzyme activity. A fluorescent reporter substrate corresponding to the P4 to P1 amino acids, RYFD, of this substrate was synthesized with a N-terminal acetyl group and C-terminal amc group. Cleavage of Ac-RYFD-amc by Tv20S was completely inhibited by bortezomib but not by RR11a. These data indicate that Ac-RYFD-amc is cleaved by Tv20S β1 and it is not a substrate for the co-purified legumain-like protease (Figure 6f).

The activity of Tv20S β1 over a concentration range of Ac-RYFD-amc was evaluated and the K_M was calculated to be 1,778 ± 274 μM. When compared to the human β1 substrate, Z-LLE-amc, Ac-RYFD-amc was less efficiently cleaved (Figure 6e), but in the presence of CP-17 and CFZ a different inhibition profile emerged for these two substates. Thus, as expected from the known inhibitory profiles of CP-17 and CFZ, 10 μM of CP-17 alone or in combination with CFZ did not inhibit cleavage of Ac-RYFD-amc substrate cleavage. In fact, subunit activity increased by 160% or more as was also seen in the MSP-MS assay with the longer substrate, EPLDLQKQ-RYFD*WL (Figure 6d). In contrast, for the human substrate Z-LLE-amc, 1 μM of CP-17 partially inhibited activity and 10 μM CP-17 completely inhibited activity (Figure 6e). These inhibition profiles suggest that Z-LLE-amc is cleaved not only by Tv20S β1, but possibly by all three catalytic subunits. In summary, Ac-RYFD-amc is a specific substrate for Tv20S β1 and therefore superior to Z-LLE-amc for identifying inhibitors that target this subunit.

2.7 | Validation of substrates with established proteasome inhibitors

To establish the utility of the newly designed Tv20S substrates for use as tools for inhibitor screening, dose–response curves were generated for all three Tv20S subunits using CP-17 and CFZ. CP-17 is a potent β5 inhibitor (IC_{50} of 94.7 ± 18.9 nM) (Figure 7a), and CFZ inhibited

β5 (IC_{50} of 78.4 ± 17.3 nM) and β2 (IC_{50} of 372.5 ± 92.1 nM) (Figure 7b). For both compounds, a concentration-dependent increase in β1 activity (>200% at the highest concentration) was measured. These subunit inhibition patterns are consistent with the decrease in probe labeling of the catalytic sites following pre-incubation with CFZ and CP-17 (Figure 2a–d). In addition, leupeptin, an inhibitor of human β2 activity (Kisselev et al. 2006) was incubated with Tv20S and then assayed with the three substrates. Leupeptin inhibited only β2 (IC_{50} of 3,159 ± 654 nM) while activating β1 (Figure 7c). Finally, ixazomib, a clinically used proteasome inhibitor for treatment of multiple myeloma (Kisselev 2022) was preincubated with Tv20S and found to inhibit Tv20S β5 (IC_{50} of 34.1 ± 5.4 nM) and β1 (IC_{50} of 269.6 ± 97.1 nM) with concomitant activation of the β2 subunit (Figure 7d). In a previous study, ixazomib had activity against trichomonads *in vitro* and *in vivo* (O'Donoghue et al. 2019), so the observed dual inhibition of β1 and β5 reveals the mechanism of action for this drug. Taken together, these analyses confirm that the new subunit specific substrates can distinguish between the three catalytic subunits and can help to define the mechanism of action of proteasome inhibitors against Tv.

2.8 | Screening of novel proteasome inhibitors for Tv20s subunit specific inhibition

To further demonstrate the utility of our new substrates, we screened a library of 284 peptide-based epoxyketone proteasome inhibitors for activity against Tv in culture. These compounds are analogs of zetomipzomib (KZR-616) and were originally developed as human immunoproteasome inhibitors for the treatment of lupus nephritis (Johnson et al. 2018; Muchamuel et al. 2023). Six of the compounds had inhibitory activities at 1 μM or less against live Tv (*i.e.*, $pEC_{50} > 6$) (Figure 8a). The top two compounds, KZR-58100 and KZR-58165, had pEC_{50} values of 6.63 ± 0.13 (EC_{50} = 230 nM) and 6.56 ± 0.21 (EC_{50} = 280 nM), respectively. Against HeLa cell lines, the compounds had pEC_{50} values of 5.12 ± 0.06 (EC_{50} = 7,510 nM) and 5.32 ± 0.1 (EC_{50} = 4,780 nM), yielding selectivity indices of 27.29 and 20.55, respectively. Both compounds consist of tripeptide-epoxyketones that differ only by the stereochemistry of alanine in the P3 position (Figure 8b). When Tv lysate was pre-incubated with these inhibitors prior to Me4BodipyFL-Ahx3-Leu3VS labeling of the subunits, the staining of the β5

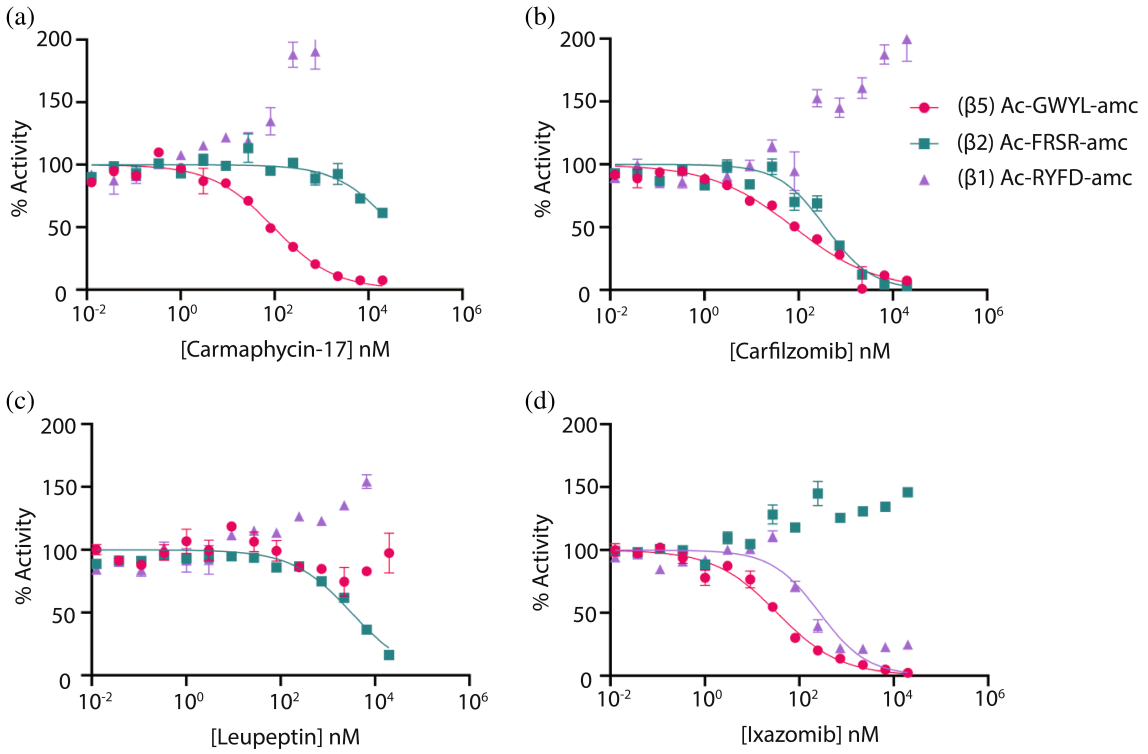

FIGURE 7 Validation of subunit-selective substrates. Concentration-response curves for Tv20S subunit inhibition by (a) CP-17, (b) CFZ, (c) leupeptin, and (d) ixazomib, with activity normalized to a 0.025% DMSO control. Assays were performed using 30 μM Ac-GWYL-amc (β5), 30 μM Ac-FRSR-amc (β2) or 50 μM Ac-RYFD-amc (β1). Fluorescence was measured over 2 h and the velocity of each reaction was plotted to generate concentration-response curves (data points show mean ± SE, n = 3 replicates). IC_{50} values were calculated by fitting to a concentration–response curve using GraphPad Prism 9.

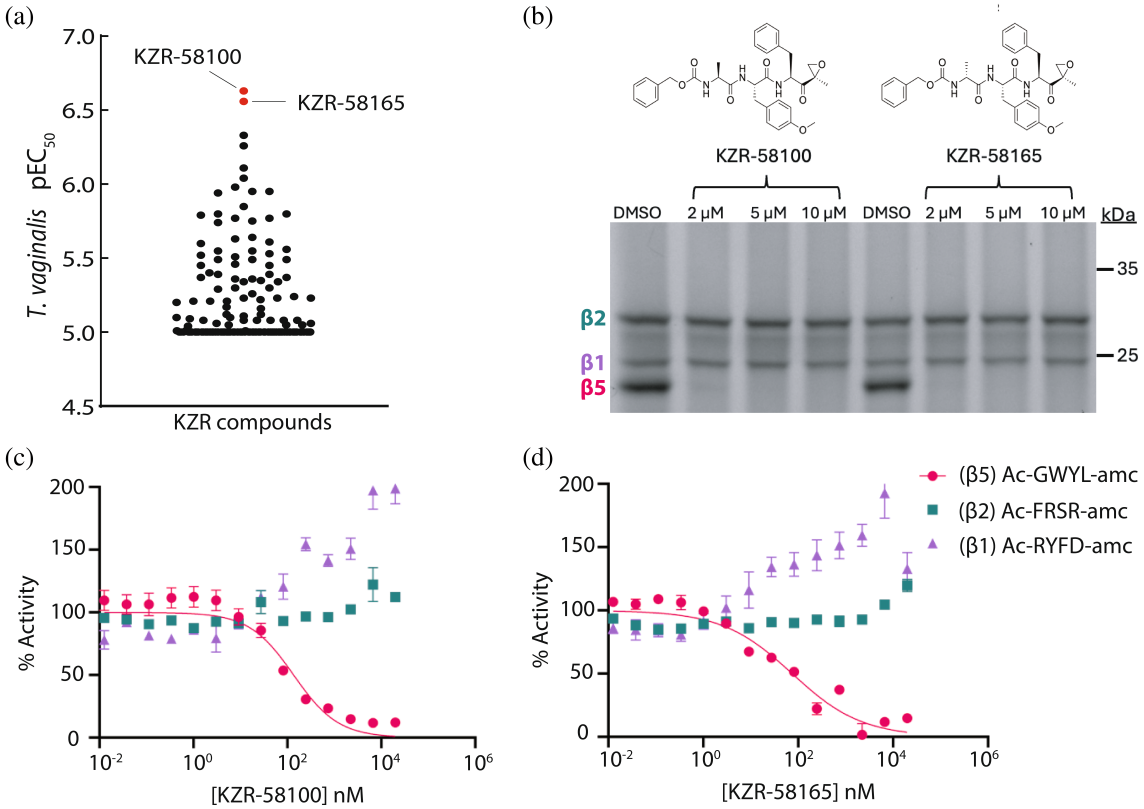

FIGURE 8 Inhibition of Tv growth by two β5 subunit specific proteasome inhibitors. (a) Whole-cell activity (EC_{50}) screen of 284 proteasome inhibitors comprising the Kezar Life Sciences library against Tv. Each data point represents the mean pEC_{50} for one compound ($n = 3$ biological replicates). The top 2 most active compounds are highlighted in red. (b) Chemical structures of KZR-58100 and KZR-58165. Subunit staining by a 24 h incubation with Me4BodipyFL-Ahx3Leu3VS following pre-incubation of Tv lysate with KZR-58100 and KZR-58165. The sample was then size-separated by SDS-PAGE. (c, d) Concentration-response curves for Tv20S subunit inhibition by KZR-58100 and KZR-58165. Activity was normalized to a 0.025% DMSO control. IC_{50} values were calculated by fitting to a dose–response curve using GraphPad Prism 9 (mean ± SE, $n = 3$ replicates).

subunit was reduced while the other subunits were unaffected (Figure 8b). Finally, these compounds were assayed with Tv20S using the newly designed β1, β2, and β5 substrates. Both KZR-58100 and KZR-58165 targeted Tv20S β5, with IC_{50} values of 136.0 ± 34.7 nM (Figure 8c) and 74.6 ± 24.3 nM (Figure 8d), respectively. Both compounds also increased β1 activity by 200% and β2 activity by 120% at the highest concentrations tested. These data suggest that the activity of KZR-58100 and KZR-58165 against Tv was mediated by inhibition of the Tv20S β5 subunit alone.

3 | DISCUSSION

This study highlights the importance of biochemically characterizing proteasome of targeted organisms as clear differences in substrate cleavage preferences exist across species. Previously, we validated the Tv20S proteasome as a druggable target using a panel of peptide inhibitors with boronic acid or epoxyketone warheads (O'Donoghue et al. 2019). However, we utilized the human proteasome substrates, which we found here to be sub-optimal reporter substrates of Tv20S activity. The current work reveals the distinct substrate preference of the catalytic Tv20S subunits. The findings allowed us to develop new reporter substrates that specifically measure the activity of each subunit, making these substrates important new tools to quantify enzyme activity of the β1, β2, and β5 subunits of Tv for detecting changes in catalytic activity in the presence of inhibitors or activators.

Key to the success of our studies was an improved protocol for isolating Tv20S from Tv lysate by using a three-step enrichment protocol that was optimized from a previously reported protocol (O'Donoghue et al. 2019). This protocol allowed us to visualize the three probe-labeled catalytic subunits on an SDS-PAGE gel and excise each band for proteomic identification. Such validation experiment would be valuable for all pathogen proteasomes that are being targeted for inhibitor development

as it is often unclear which band corresponds to which subunit. For example, when *Plasmodium falciparum* 20S was labeled with a fluorescent probe, MV151, the upper and lower bands were designated as β5 and β2, respectively, while the β1 subunit was not labeled (Li et al. 2014). However, in a follow-up study by the same group with a new probe (BMV037) that labels all three subunits, the upper, middle and lower bands were designated as β1, β2 and β5, respectively (Li et al. 2016). Thus, for *P. falciparium*, clear consensus remains elusive as to which labeled band corresponds to which subunit. By taking the approach outlined here, which involves enriching the proteasome from cell extracts and performing proteomic analysis on the excised bands illuminated with the probe, definitive identification of each subunit was possible.

Previously, Tv was screened against a library of proteasome inhibitors derived from the marine natural product, carmaphycin B (O'Donoghue et al. 2019). The leading compound, carmaphycin-17 (CP-17), was more effective than metronidazole at killing Tv *in vitro* as well as *in vivo* using a murine model infected with the related parasite, *Tritrichomonas foetus*. Importantly, CP-17 could overcome metronidazole resistance and was found to directly target the Tv20S proteasome (O'Donoghue et al. 2019). CP-17 also showed >5-fold greater potency to Tv20S proteasome than human proteasome and less cytotoxicity to HeLa cells compared to anticancer proteasome inhibitors. There is low sequence conservation between human and trichomonad catalytic subunits (28%–52% sequence identity) which would indicate that inhibitors with improved selectivity could be designed. We and others have developed proteasome inhibitors that are >2,000-fold more toxic to *Plasmodium falciparum* than human cells (LaMonte et al. 2017; Zhang et al. 2022) and therefore there is potential for developing Tv-specific proteasome inhibitors that could reach the same level of selectivity. However, unlike the Plasmodium research, little is known about the catalytic subunits of Tv20S and the fluorogenic reporter substrates that have been used in the past, were developed for the human proteasome. To advance Tv proteasome inhibitor development, it is important that optimal reporter substrates are developed to quantify inhibition of β1, β2, and β5. To do this, then the substrate specificity profile for each subunit needs to be uncovered.

Several methods have been used to uncover the substrate specificity of the human proteasome. Harris and colleagues incubated the human 20S proteasome with a combinatorial library of tetrapeptides containing a C-terminal fluorogenic reporter group (Harris et al. 2001) and used these data to develop a panel of substrates that are efficiently cleaved. However, it was not confirmed which catalytic subunit was responsible for cleaving each substrate. In another study, Rut and colleagues used a much larger library of tetrapeptides containing natural and non-natural amino to generate substrate specificities of each catalytic subunit. In this case, they used three sub-libraries that had either Asp, Arg or Ala fixed in the P1 position to preference cleavage by β1, β2, or β5, respectively (Rut et al. 2018). To validate the hit substrates, they synthesized three fluorogenic substrates consisting of peptide sequences that were specific for each of the three subunits making these substrates valuable for screening human proteasome inhibitors, similar to what we found for the Tv specific substrates.

We previously used MSP-MS to uncover the substrate specificity of the human and *Plasmodium* proteasomes (Li et al. 2016; Winter et al. 2017). The method utilizes a library of 228 strategically designed synthetic 14-mer peptides as substrates for proteases, where cleavage of each substrate can be quantified by LC–MS/MS. In studies with human and Plasmodium proteasomes we obtained substrate profiles for the whole proteasome but were unable to determine which subunits were responsible for cleaving each peptide. Therefore, in this study, we sought to use the MSP-MS method to generate a substrate specificity profile of each catalytic subunit of Tv20S. As proteasome subunits cannot be physically separated from each other, we took a chemical approach to inactivate one or two subunits of Tv20S and then generate a substrate specificity profile for the subunit(s) that still retain activity. More specifically, we inactivated β5 alone using CP-17 and β5 + β2 with a mixture of CP-17 and CFZ. While other proteasome inhibitors are known to target β2 (*e.g.*, leupeptin) and β5 + β1 (*e.g.*, bortezomib), none of these compounds bind irreversible to the proteasome and therefore it is possible that the inhibitors may dissociate for the target subunit during the incubation with peptide library, which could ultimately lead to spurious data.

Studies with CP-17 and CFZ identified three groups of cleaved peptides which correlated with the three catalytic subunits. From here, representative peptides from each group were chosen and fluorogenic reporter substrates were designed. The β5 and β2 substrates, namely Ac-GWYL-amc and Ac-FRSR-amc, had lower K_M values when compared to the commercially available substrates, Suc-LLVY-amc (for β5) and Boc-LRR-amc (for β2) that are commonly used for detecting human and microbial proteasome activities (Andersson et al. 1998; Bonet-Costa et al. 2019; Ott et al. 2021). In general, the limiting reagent in parasite proteasome assays is the amount of enzyme available. Therefore, having substrates that are efficiently cleaved by Tv20S will allow for more screening studies and dose–response assays.

When assessing the peptides cleaved in Group 3, we found that many cleaved products were not inhibited by CP-17 and CFZ and some products were increased by up

to 400% when compared to the untreated sample. In addition, a strong preference for cleaving peptides after Asn residues was unusual, as the β1 subunits in proteasomes from other organisms generally cleave after Glu, Asp and Leu (Tanaka 2009). We subsequently determined that the enzyme responsible for cleaving after Asn was a legumain-like protease(s) that co-purified with Tv20S. Co-purification of other proteases with the proteasome has been reported previously (Thibaudeau and Smith 2019). For example, tripeptidyl peptidase II (TPPII) co-purified with the mouse proteasome from EL4 cells (T lymphoblast; mouse) following ultra-centrifugation and anion exchange chromatography (Geier et al. 1999). This led the authors to conclude that TPPII provides additional proteolytic capabilities for the mouse proteasome. While TPPII is a large protease with a MW of 138 kDa, legumain-like proteases such as TvLEGU-1 are predicted to be only ~30 kDa (Ekici et al. 2004; Götz et al. 2008; León-Félix et al. 2004; Rendón-Gandarilla et al. 2013). Therefore, this enzyme should not elute from the size exclusion column in the same fraction as the 700 kDa proteasome, leading us to hypothesize that it may directly bind to the proteasome. If so, the function of legumain may provide the proteasome with additional specificity for cleaving after Asn residues.

When comparing the inhibition profile of the new Tv20S β1 substrate, Ac-RYFD-amc, with the commercial β1 substrate Z-LLE-amc it was clear that they are not cleaved by the same subunit. Using Ac-RYFD-amc, β1 activity increased by 160% in the presence of 10 μM CP-17, however, under the same conditions, Tv20S activity using Z-LLE-amc was fully inhibited. Based on the activity of Tv20S with Z-LLE-amc in the presence of different inhibitors, it is likely that all three subunits of Tv20S are capable of cleaving Z-LLE-amc. While this substrate is not suitable to evaluate Tv20S β1 activity it can still be a useful reagent to detect Tv20S activity in Tv extracts and track proteasome activity in chromatography fractions during the purification procedure. This discovery highlights the importance of developing parasite-specific reporter substrates, as the widely available human proteasome substrates may not be cleaved by the intended subunit.

Armed with three new subunit selective substrates, we validated their use in identifying the mechanism of action of different inhibitors. Consistent with our previous study CP-17 was selective for Tv20S β5 and inhibited β2 at higher concentrations, whereas CFZ inhibited both β5 and β2 (O'Donoghue et al. 2019). Ixazomib targeted β5 and β1 and caused an increase in β2 activity while leupeptin inhibited β2 and increased activity of β1. Inhibition of some subunits that results in the concomitant increase in activity of another suggests that the functioning of the β1, β2, and β5 subunits are intricately linked. The β1 and β2 subunits of Tv20S are predicted to be adjacent on the β ring and therefore binding of an inhibitor to one subunit may directly affect substrate access to the adjacent subunit. However, it is unclear how inhibition of β5 increases activity of β1 since they are predicted to be one opposite sides of the β ring. Proteasomes first assemble into half-proteasomes consisting of one α-ring and one β-ring. Two β-rings from these half-proteasomes then combine to form the 20S enzyme complex (Adolf et al. 2024). It is possible the β5 from one half-proteasome binds close to the β1 from the second half-proteasome, which could then result in β5 inhibition being able to modulate β1 activity. For future studies, it will be important to understand the cellular implications of inhibiting one or more subunits of the proteasome, while simultaneously activating another subunit.

Finally, we tested our substrates using two new inhibitors, KZR-58100 and KZR-58165, that are potent anti-parasitic agents for Tv in culture. These compounds are analogs of zetomipzomib (KZR-616), an immunoproteasome-selective inhibitor in clinical trials for treatment of lupus nephritis (Johnson et al. 2018; Muchamuel et al. 2023). KZR-616 targets all three subunits of the human immunoproteasome, however the two analogs tested inhibit only the β5 subunit of Tv20S with IC_{50} values of 136.0 ± 34.7 nM and 74.6 ± 24.3 nM. These compounds reveal that the anti-parasitic effects of proteasome inhibitors can be mediated through inhibition of the β5 subunit alone. These compounds can be a starting point for development of a series of Tv20S inhibitors that have greater selectivity for Tv over human cells, as we have achieved for *P. falciparum*-specific inhibitors (Almaliti et al. 2023).

To summarize, our improved proteasome isolation protocol for Tv20S and the application of substrate cleavage profiling yielded subunit selective substrates with which the respective catalytic activities of Tv20S can be individually evaluated. The approach outlined here is applicable to any new proteasome of interest as the standard commercial substrates may be sub-optimal or non-specific for the target subunits of particular organisms. The tools developed in this study will also aid in our understanding of the biological functions of the Tv20S and allow us to understand the mechanism of action for all new inhibitors that are developed to treat trichomoniasis.

4 | EXPERIMENTAL PROCEDURES

4.1 | *Trichomonas vaginalis* cell culture

Tv F1623 (Brown et al. 1999) parasites were cultured in TYM (trypticase, yeast extract, and maltose). Diamond's medium supplemented with 180 mM ferrous ammonium

sulfate. Cells were maintained at 37°C under anaerobic conditions (AnaeroPack-Anaero system).

4.2 | Purification of native Tv20S

Tv20S proteasome was purified from frozen pellets of Tv parasites using a modification of published procedure (O'Donoghue et al. 2019). Briefly, frozen pellets of washed parasites in 50 mM HEPES, pH 7.5, 10 mM E-64, were thawed on ice and resuspended in 1 mL of lysis buffer containing 50 mM HEPES, pH 7.5, 10 mM E-64, 100 mM AEBSF, 1 mM pepstatin A, and 1 mM dithiothreitol (DTT) and sonicated three times on ice. The lysate was clarified by centrifugation at 30,000 *g* for 20 min. The 20S proteasome was precipitated with 30% and 60% ammonium sulfate and collected by centrifugation (30,000 *g*, 30 min). The pellet was resuspended in 50 mM HEPES, pH 7.5, 125 mM NaCl, and purified by gel filtration using a Superose 6 Increase column (GE Healthcare). Fractions containing enzyme that cleaved Suc-LLVY-amc and were sensitive to 10 μM CFZ were pooled. The pooled fractions were applied to a 5 mL HiTrap DEAE FF column (GE Healthcare), and washed with 50 mM Tris–HCl, pH 7.5. Tv20S proteasome was eluted using a 0–1 M NaCl gradient in 50 mM Tris–HCl, pH 7.5. Fractions containing proteasome activity were pooled, buffer exchanged to 50 mM HEPES, pH 7.5, aliquoted and stored at −80°C.

4.3 | Protein gels

Tv20S and c20S were diluted with 50 mM HEPES pH 7.5 then mixed with 2 μM of Me4BodipyFL-Ahx3Leu3VS (R&D Systems #I-190). Tv lysate was first diluted with 50 mM HEPES pH 7.5 and 10 μM E64 before 2 μM of probe was added. After probe addition, samples were incubated at 37°C for up to 24 h. For denaturing gels, samples were mixed with 4X Bolt LDS sample buffer (Thermo Fisher Scientific) containing DTT, incubated at 99°C for 5 min and loaded into a Bolt 4%–12% Bis-Tris (Thermo Fisher Scientific) or NuPAGE 12% Bis-Tris (Thermo Fisher Scientific) alongside PageRuler Plus pre-stained protein ladder (Thermo Fisher Scientific). Gels were run with 1X MES or 1X MOPS SDS buffers (Invitrogen) at 130 V. For native gels, samples were mixed with 2X Novex Tris-glycine native sample buffer and loaded into NuPage Tris-glycine gels (Invitrogen) with NativeMark unstained protein standard (Thermo Fisher Scientific). Gels were run at 130 V with Novex Tris-glycine running buffer (Invitrogen). All gels were imaged on Bio-Rad ChemiDoc XRS+ at 470 nm excitation 530 nm emission for probe visualization and imaged with white light for silver stain visualization. Silver stain was performed using Pierce™ Silver Stain Kit (Thermo Fisher Scientific). Probe labeled bands were quantified using ImageJ from three independent experiments (Schneider et al. 2012).

4.4 | Liquid chromatography with tandem mass spectrometry (LC–MS/MS)

Gel bands were excised from a denaturing gel using a clean scapel. The digestion protocol and LC–MS/MS instrumentation set up was as previously reported (Røyseth et al. 2023). Resulting data was searched against the *Trichomonas vaginalis* proteome (UniProt taxon ID 412133) using PEAKS studio (v8.5) software (Bioinformatics Solutions Inc.) with a precursor mass error tolerance of 20 ppm and fragment mass error tolerance of 0.01 Da defined and trypsin digest specified. The identified peptides were adjusted to a false discovery rate of <1%. The intensity of all proteins found in each band was totaled as was the intensity of all non-catalytic proteasome subunits (UniProt Accession numbers: A2D8G5, A2FCM7, A2FT79, A2E1I9, A2DTN3, A2FJV7, A2F568, A2F3X4, A2F8W4, A2F716, A2F3H9). A sum of intensities of all 14 proteasome subunits was subtracted from total protein intensity to determine intensity of other proteins in the sample. The data was analyzed as a pie chart in GraphPad Prism 9 (GraphPad Software).

4.5 | Preparation of substrate and inhibitors

Carfilzomib (CFZ), E64, AEBSF, Pepstatin A, and Z-AAN-amc were purchased from MedChemExpress. Suc-LLVY-amc, Boc-LRR-amc, and Z-LLE-amc were purchased from Cayman Chemical. Newly designed substrates were custom synthesized by GenScript and dissolved in DMSO to 10 mM (Ac-GWYL-amc, Ac-FRSR-amc, Ac-PSRN-amc) or 50 mM (Ac-RYFD-amc). HPLC and mass spectrometry data for the new substrates can be found in Data S2. Substrates were dissolved in DMSO at a concentration of 10 mM and stored at −20°C (Ac-GWYL-amc, Ac-FRSR-amc) or −80°C (Ac-RYFD-amc). Inhibitors were dissolved in DMSO to 10 mM and serially diluted in DMSO on a black 384-well microplates. Inhibitors and substrates were transferred using an acoustic transfer system (Biosera) into low volume 384-well microplates as needed.

4.6 | Multiplex substrate profiling by mass spectrometry (MSP-MS)

Tv20S was pre-incubated with CP-17, CFZ, or DMSO prior to mixing with an equimolar mixture of 228 14-mer peptides such that the final concentration of each peptide was 0.5 μM and the final concentration of inhibitor was either 1 μM (CP-17) or 10 μM (CP-17 and CFZ). The exact concentration of Tv20S was unknown due to levels being below the detection limit for protein quantification kits, such as a BCA assay. However, a 1:20 dilution of the enzyme stock was used. Reactions were incubated at room temperature and after 3, 20, and 38 h, 10 μL of this mixture was removed and the enzyme inactivated by mixing with 40 μL of 8M urea. A 0 h timepoint was generated by first mixing 5 μL of inhibitor/enzyme with 40 μL of 8M urea, incubating for 20 min, then adding 5 μL of peptide mix. The reactions were performed in quadruplicate reaction tubes in assay buffer consisting of 50 mM HEPES pH 7.5, 10 μM E64, 100 μM AEBSF, 10 μM pepstatin, 1 mM DTT. The samples were then desalted, prepared for mass spectrometry, and analyzed as previously described (Almaliti et al. 2023), including iceLogo generation (Colaert et al. 2009).

4.7 | Hierarchical clustering analysis

Clustering of peptides sequences and their cleavage patterns were assessed by hierarchical cluster analysis (HCA) with the ArrayTrack™ bioinformatics tool from the National Center for Toxicological Research (NCTR), Food and Drug Administration (FDA) (Xu et al. 2010). ArrayTrack™ is a minimum information about a microarray experiment (MIAME) supportive tool, which provides linking between results with functional information and a given method (*i.e.*, data biological relevance). HCA allows investigating grouping of samples or any data elements by their similarity profiles. Analysis was performed employing the dual cluster method, with Euclidean metric for distance measurements, and Ward's linkage type.

4.8 | Kinetic Tv20S assays and inhibitor screening

Activity assays were performed by diluting Tv20S 1:20 in assay buffer (50 mM HEPES pH 7.5, 10 μM E64, 100 μM AEBSF, 10 μM pepstatin, 1 mM DTT) with the indicated substrate. For substrate validation assays a final volume of 30 μL per well was used in black 384-well plates (Thermo Scientific #262260). IC_{50} curves were generated with 7.5 mL final volume on 384-well low volume black microplates (Greiner Bio-One #784900). Fluorescence was measured for 2 h at excitation 360 nm and emission of 460 nm on a Synergy HTX Multi-Mode Microplate Reader (BioTek). Z-AAN-amc, Suc-LLVY-amc, Boc-LLR-amc, and Z-LLE-amc were purchased from MedChemExpress.

4.9 | Whole cell activity assays against Tv

The antitrichomonal activity against Tv F1623 was assessed as described previously (O'Donoghue et al. 2019). Cells were grown at 37°C in TYM Diamond's medium supplemented with 180 μM ferrous ammonium sulfate. Briefly, stocks of the test compounds were diluted in 0.1 μL of dimethyl sulfoxide (DMSO) to 2 mM, and 1:3 serial dilutions were made in 384-well microplates using Acoustic Liquid Dispenser (EDC Biosystems). A 20 μL trophozoites suspension (10^3/well) in TYM was added to each well with diluted compounds, and cultures were incubated for 24 h at 37°C under anaerobic conditions (AnaeroPack-Anaero system). Growth and viability were determined with an ATP assay by adding BacTiter-Glo microbial cell viability assay reagent (Promega) and by measuring ATP-dependent luminescence in a Spectra Max M2E microplate reader (Molecular Devices). The 50% effective concentration (EC_{50}) was derived from the concentration-response curves using GraphPad Prism 9 (GraphPad Software).

AUTHOR CONTRIBUTIONS

Pavla Fajtova: Conceptualization; data curation; formal analysis; funding acquisition; investigation; validation; visualization; writing – original draft; writing – review and editing. **Brianna M. Hurysz:** Conceptualization; investigation; writing – original draft; validation; visualization; formal analysis; data curation; writing – review and editing. **Yukiko Miyamoto:** Investigation; visualization. **Mateus Sá M. Serafim:** Investigation; visualization; methodology. **Zhenze Jiang:** Software; methodology. **Julia M. Vazquez:** Investigation. **Diego F. Trujillo:** Investigation. **Lawrence J. Liu:** Investigation. **Urvashi Somani:** Investigation. **Jehad Almaliti:** Resources. **Samuel A. Myers:** Resources. **Conor R. Caffrey:** Writing – review and editing; conceptualization; funding acquisition; supervision. **William H. Gerwick:** Writing – review and editing; supervision. **Dustin L. McMinn:** Resources. **Christopher J. Kirk:** Resources. **Evzen Boura:** Funding acquisition; supervision. **Lars Eckmann:** Conceptualization; writing – review and editing; supervision; funding acquisition. **Anthony J. O'Donoghue:** Writing – original draft; funding

acquisition; project administration; supervision; visualization; conceptualization; validation; writing – review and editing.

ACKNOWLEDGMENTS

J.A. acknowledges the deanship of scientific research at the University of Jordan for the scientific leave. The research was supported by NIH awards R01 AI158612 and R21 AI146387 to A.J.O. and L.E., R21 AI133393 and R21 AI171824 to A.J.O. and C.R.C., and DK120515 to L. E. The content is solely the responsibility of the authors and does not necessarily represent the official views of the National Institutes of Health. P.F. received funding from the Programme for Research and Mobility Support of Starting Researchers from the Czech Academy of Sciences (MSM200551901) and the European Union's Horizon 2020 research and innovation program under the Marie Skłodowska-Curie grant agreement No. 846688, ProTeCT. B.M.H. and D.F.T. were supported in part by the University of California-San Diego (UCSD) Graduate Training Program in Cellular and Molecular Pharmacology through an institutional training grant from the National Institute of General Medical Sciences, T32GM007752. J.A. would like to acknowledge the St. Baldrick's Foundation for the International Scholar award 2022–2025. M.S.M.S. was funded by the CAPES foundation (Brazil), grant numbers 88887.595578/2020-00 and 88887.684031/2022-00, and UFMG intramural funds.

CONFLICT OF INTEREST STATEMENT

The authors declare no conflicts of interest.

DATA AVAILABILITY STATEMENT

The MSP-MS data are available publicly (ftp://massive.ucsd.edu/v02/MSV000093794 or ProteomeXchange PXD048324). The LC–MS/MS data for the in-gel digest of individual subunits is also available publicly (ftp://massive.ucsd.edu/v01/MSV000092082 or ProteomeXchange PXD042632). Processed MSP-MS data can be found in Data S3.

ORCID

Anthony J. O'Donoghue https://orcid.org/0000-0001-5695-0409

REFERENCES

Adolf F, Du J, Goodall EA, Walsh RM, Rawson S, von Gronau S, et al. Visualizing chaperone-mediated multistep assembly of the human 20S proteasome. Nat Struct Mol Biol. 2024;31:1176–88. https://doi.org/10.1038/s41594-024-01268-9

Almaliti J, Fajtová P, Calla J, LaMonte GM, Feng M, Rocamora F, et al. Development of potent and highly selective Epoxyketone-based plasmodium proteasome inhibitors. Chemistry (Weinheim an Der Bergstrasse, Germany). 2023;29(20):e202203958. https://doi.org/10.1002/chem.202203958

Andersson M, Sjøstrand J, Karlsson JO. Proteolytic cleavage of N-Succ-Leu-Leu-Val-Tyr-AMC by the proteasome in lens epithelium from clear and cataractous human lenses. Exp Eye Res. 1998;67:231–6.

Becker SH, Darwin KH. Bacterial proteasomes: mechanistic and functional insights. Microbiol Mol Biol Rev. 2016;81:e00036-16.

Berkers CR, van Leeuwen FWB, Groothuis TA, Peperzak V, van Tilburg EW, Borst J, et al. Profiling proteasome activity in tissue with fluorescent probes. Mol Pharm. 2007;4:739–48.

Bibo-Verdugo B, Jiang Z, Caffrey CR, O'Donoghue AJ. Targeting proteasomes in infectious organisms to combat disease. FEBS J. 2017;284:1503–17.

Bibo-Verdugo B, Wang SC, Almaliti J, Ta AP, Jiang Z, Wong DA, et al. The proteasome as a drug target in the metazoan pathogen, *Schistosoma mansoni*. ACS Infect Dis. 2019;5:1802–12.

Bonet-Costa V, Sun PY, Davies KJA. Measuring redox effects on the activities of intracellular proteases such as the 20S proteasome and the immuno-proteasome with fluorogenic peptides. Free Radic Biol Med. 2019;143:16–24.

Brown DM, Upcroft JA, Dodd HN, Chen N, Upcroft P. Alternative 2-keto acid oxidoreductase activities in *Trichomonas vaginalis*. Mol Biochem Parasitol. 1999;98:203–14.

Buac D, Shen M, Schmitt S, Kona FR, Deshmukh R, Zhang Z, et al. From Bortezomib to other inhibitors of the proteasome and beyond. Curr Pharm des. 2013;19:4025–38.

Budenholzer L, Cheng CL, Li Y, Hochstrasser M. Proteasome structure and assembly. J Mol Biol. 2017;429:3500–24.

Cates W. Estimates of the incidence and prevalence of sexually transmitted diseases in the United States. American Social Health Association Panel. Sex Transm Dis. 1999;26:S2–7.

Colaert N, Helsens K, Martens L, Vandekerckhove J, Gevaert K. Improved visualization of protein consensus sequences by iceLogo. Nat Methods. 2009;6:786–7.

Collins GA, Goldberg AL. The logic of the 26S proteasome. Cell. 2017;169:792–806.

Collins GA, Gomez TA, Deshaies RJ, Tansey WP. Combined chemical and genetic approach to inhibit proteolysis by the proteasome. Yeast. 2010;27:965–74.

Cudmore SL, Delgaty KL, Hayward-McClelland SF, Petrin DP, Garber GE. Treatment of infections caused by metronidazole-resistant trichomonas vaginalis. Clin Microbiol Rev. 2004;17:783–93.

Dingsdag SA, Hunter N. Metronidazole: an update on metabolism, structure–cytotoxicity and resistance mechanisms. J Antimicrob Chemother. 2018;73:265–79.

Ekici OD, Götz MG, James KE, Li ZZ, Rukamp BJ, Asgian JL, et al. Aza-peptide Michael acceptors: a new class of inhibitors specific for caspases and other clan CD cysteine proteases. J Med Chem. 2004;47:1889–92.

Geier E, Pfeifer G, Wilm M, Lucchiari-Hartz M, Baumeister W, Eichmann K, et al. A giant protease with potential to substitute for some functions of the proteasome. Science. 1999;283:978–81.

Götz MG, James KE, Hansell E, Dvorák J, Seshaadri A, Sojka D, et al. Aza-peptidyl Michael acceptors. A new class of potent and selective inhibitors of asparaginyl endopeptidases (legumains)

from evolutionarily diverse pathogens. J Med Chem. 2008;51:2816–32.

Harris JL, Alper PB, Li J, Rechsteiner M, Backes BJ. Substrate specificity of the human proteasome. Chem Biol. 2001;8:1131–41.

Hernández Ceruelos A, Romero-Quezada LC, Ruvalcaba Ledezma JC, López Contreras L. Therapeutic uses of metronidazole and its side effects: an update. Eur Rev Med Pharmacol Sci. 2019;23:397–401.

Huang C, Feng S, Huo F, Liu H. Effects of four antibiotics on the diversity of the intestinal microbiota. Microbiol Spectrum. 2022;10:e01904-21.

Jalovecka M, Hartmann D, Miyamoto Y, Eckmann L, Hajdusek O, O'Donoghue AJ, et al. Validation of Babesia proteasome as a drug target. Int J Parasitol Drugs Drug Resist. 2018;8:394–402.

Johnson HWB, Lowe E, Anderl JL, Fan A, Muchamuel T, Bowers S, et al. Required immunoproteasome subunit inhibition profile for anti-inflammatory efficacy and clinical candidate KZR-616 ((2S,3R)-N-((S)-3-(Cyclopent-1-en-1-yl)-1-((R)-2-methyloxiran-2-yl)-1-oxopropan-2-yl)-3-hydroxy-3-(4-methoxyphenyl)-2-((S)-2-(2-morpholinoacetamido)propanamido)propenamide). J Med Chem. 2018;61:11127–43.

Kisselev AF. Site-specific proteasome inhibitors. Biomolecules. 2022;12:54.

Kisselev AF, Callard A, Goldberg AL. Importance of the different proteolytic sites of the proteasome and the efficacy of inhibitors varies with the protein substrate. J Biol Chem. 2006;281:8582–90.

Kissinger P. Trichomonas vaginalis: a review of epidemiologic, clinical and treatment issues. BMC Infect Dis. 2015;15:307.

Koester DC, Marx VM, Williams S, Jiricek J, Dauphinais M, René O, et al. Discovery of novel quinoline-based proteasome inhibitors for human African trypanosomiasis (HAT). J Med Chem. 2022;65:11776–87.

Krishnan KM, Williamson KC. The proteasome as a target to combat malaria: hits and misses. Transl Res. 2018;198:40–7.

LaMonte GM, Almaliti J, Bibo-Verdugo B, Keller L, Zou BY, Yang J, et al. Development of a potent inhibitor of the Plasmodium proteasome with reduced mammalian toxicity. J Med Chem. 2017;60:6721–32.

Lapek JD, Jiang Z, Wozniak JM, Arutyunova E, Wang SC, Lemieux MJ, et al. Quantitative multiplex substrate profiling of peptidases by mass spectrometry. Mol Cell Proteomics. 2019;18:968–81.

León-Félix J, Ortega-López J, Orozco-Solís R, Arroyo R. Two novel asparaginyl endopeptidase-like cysteine proteinases from the protist *Trichomonas vaginalis*: their evolutionary relationship within the clan CD cysteine proteinases. Gene. 2004;335:25–35.

Li H, O'Donoghue A, van der Linden W, et al. Structure- and function-based design of Plasmodium-selective proteasome inhibitors. Nature. 2016;530(7589):233–6. https://doi.org/10.1038/nature16936

Li H, Tsu C, Blackburn C, Li G, Hales P, Dick L, et al. Identification of potent and selective non-covalent inhibitors of the *Plasmodium falciparum* proteasome. J Am Chem Soc. 2014;136:13562–5.

Liggett A, Crawford LJ, Walker B, Morris TCM, Irvine AE. Methods for measuring proteasome activity: current limitations and future developments. Leuk Res. 2010;34:1403–9.

Manasanch EE, Orlowski RZ. Proteasome inhibitors in cancer therapy. Nat Rev Clin Oncol. 2017;14:417–33.

Menezes CB, Frasson AP, Tasca T. Trichomoniasis—Are we giving the deserved attention to the most common non-viral sexually transmitted disease worldwide? Microb Cell. 2016;3:404–19.

Muchamuel T, Fan RA, Anderl JL, Bomba DJ, Johnson HWB, Lowe E, et al. Zetomipzomib (KZR-616) attenuates lupus in mice via modulation of innate and adaptive immune responses. Front Immunol. 2023;14:1043680.

Nagle A, Biggart A, Be C, Srinivas H, Hein A, Caridha D, et al. Discovery and characterization of clinical candidate LXE408 as a kinetoplastid-selective proteasome inhibitor for the treatment of leishmaniases. J Med Chem. 2020a;63:10773–81.

Nagle A, Biggart A, Be C, Srinivas H, Hein A, Caridha D, et al. Discovery and characterization of clinical candidate LXE408 as a Kinetoplastid-selective proteasome inhibitor for the treatment of leishmaniases. J Med Chem. 2020b;63(19):10773–81.

Narcisi EM, Secor WE. In vitro effect of tinidazole and furazolidone on metronidazole-resistant trichomonas vaginalis. Antimicrob Agents Chemother. 1996;40:1121–5.

O'Donoghue AJ, Bibo-Verdugo B, Miyamoto Y, Wang SC, Yang JZ, Zuill DE, et al. 20S proteasome as a drug target in trichomonas vaginalis. Antimicrob Agents Chemother. 2019;63:e00448-19.

Ott C, Tomasina F, Campolo N, Bartesaghi S, Mastrogiovanni M, Leyva A, et al. Decreased proteasomal cleavage at nitrotyrosine sites in proteins and peptides. Redox Biol. 2021;46:102106.

Petrin D, Delgaty K, Bhatt R, Garber G. Clinical and microbiological aspects of trichomonas vaginalis. Clin Microbiol Rev. 1998;11:300–17.

Pilla R, Gaschen FP, Barr JW, Olson E, Honneffer J, Guard BC, et al. Effects of metronidazole on the fecal microbiome and metabolome in healthy dogs. J Vet Intern Med. 2020;34:1853–66.

Piro E, Kropp M, Cantaffa R, Lamberti AG, Carillio G, Molica S. Visceral leishmaniasis infection in a refractory multiple myeloma patient treated with bortezomib. Ann Hematol. 2012;91:1827–8.

Rendón-Gandarilla FJ, de Ramón-Luing AL, Ortega-López J, Rosa de Andrade I, Benchimol M, Arroyo R. The TvLEGU-1, a legumain-like cysteine proteinase, plays a key role in *Trichomonas vaginalis* cytoadherence. Biomed Res Int. 2013;2013:1–18.

Reynolds JM, El Bissati K, Brandenburg J, Günzl A, Mamoun CB. Antimalarial activity of the anticancer and proteasome inhibitor bortezomib and its analog ZL3B. BMC Clin Pharmacol. 2007;7:13.

Rohweder PJ, Jiang Z, Hurysz BM, O'Donoghue AJ, Craik CS. Multiplex substrate profiling by mass spectrometry for proteases. Methods in enzymology. Volume 682. Amsterdem: Academic Press; 2022. p. 375–411. https://doi.org/10.1016/bs.mie.2022.09.009

Rowley J, Vander Hoorn S, Korenromp E, Low N, Unemo M, Abu-Raddad LJ, et al. Chlamydia, gonorrhoea, trichomoniasis and syphilis: global prevalence and incidence estimates, 2016. Bull World Health Organ. 2019;97:548–62.

Røyseth V, Hurysz BM, Kaczorowska A-K, Dorawa S, Fedøy A-E, Arsın H, et al. Activation mechanism and activity of globupain, a thermostable C11 protease from the Arctic Mid-Ocean ridge hydrothermal system. Front Microbiol. 2023;14:1199085.

Rut W, Poręba M, Kasperkiewicz P, Snipas SJ, Drąg M. Selective substrates and activity-based probes for imaging of the human constitutive 20S proteasome in cells and blood samples. J Med Chem. 2018;61(12):5222–34. https://doi.org/10.1021/acs.jmedchem.8b00026

Saha A, Oanca G, Mondal D, Warshel A. Exploring the proteolysis mechanism of the proteasomes. J Phys Chem B. 2020;124:5626–35.

Schneider CA, Rasband WS, Eliceiri KW. NIH image to ImageJ: 25 years of image analysis. Nat Methods. 2012;9:671–5.

Schwebke JR, Barrientes FJ. Prevalence of trichomonas vaginalis isolates with resistance to metronidazole and tinidazole. Antimicrob Agents Chemother. 2006;50:4209–10.

Schwebke JR, Burgess D. Trichomoniasis. Clin Microbiol Rev. 2004;17:794–803.

Tanaka K. The proteasome: overview of structure and functions. Proc Jpn Acad Ser B Phys Biol Sci. 2009;85:12–36.

Thibaudeau TA, Smith DM. A practical review of proteasome pharmacology. Pharmacol Rev. 2019;71:170–97.

Vigneron N, Van den Eynde BJ. Proteasome subtypes and regulators in the processing of antigenic peptides presented by class I molecules of the major histocompatibility complex. Biomolecules. 2014;4(4):994–1025.

Winter MB, La Greca F, Arastu-Kapur S, Caiazza F, Cimermancic P, Buchholz TJ, et al. Immunoproteasome functions explained by divergence in cleavage specificity and regulation. eLife. 2017;6:e27364.

Wyllie S, Brand S, Thomas M, De Rycker M, Chung C, Pena I, et al. Preclinical candidate for the treatment of visceral leishmaniasis that acts through proteasome inhibition. Proc Natl Acad Sci. 2019a;116:9318–23.

Wyllie S, Brand S, Thomas M, De Rycker M, Chung C, Pena I, et al. Preclinical candidate for the treatment of visceral leishmaniasis that acts through proteasome inhibition. Proc Natl Acad Sci. 2019b;116(19):9318–23.

Xie SC, Dick LR, Gould A, Brand S, Tilley L. The proteasome as a target for protozoan parasites. Expert Opin Ther Targets. 2019;23:903–14.

Xu J, Kelly R, Fang H, Tong W. ArrayTrack: a free FDA bioinformatics tool to support emerging biomedical research—an update. Hum Genomics. 2010;4:428–34.

Zhang H, Ginn J, Zhan W, Liu YJ, Leung A, Toita A, et al. Design, synthesis, and optimization of macrocyclic peptides as species-selective Antimalaria proteasome inhibitors. J Med Chem. 2022;65(13):9350–75. https://doi.org/10.1021/acs.jmedchem.2c00611

Zhang H, Lin G. Microbial proteasomes as drug targets. PLoS Pathog. 2021;17:e1010058.

SUPPORTING INFORMATION

Additional supporting information can be found online in the Supporting Information section at the end of this article.

How to cite this article: Fajtova P, Hurysz BM, Miyamoto Y, Serafim MSM, Jiang Z, Vazquez JM, et al. Distinct substrate specificities of the three catalytic subunits of the *Trichomonas vaginalis* proteasome. Protein Science. 2024;33(12):e5225. https://doi.org/10.1002/pro.5225